fac versus *mer* Coordination for a Tridentate Diethylene Glycolate Ligand in Tantalum Complexes: A Combined Experimental and Theoretical Study

Carles Bo,[‖] Rosa Fandos,[†] Marta Feliz,[‖] Carolina Hernández,[†] Antonio Otero,*[,‡] Ana Rodríguez,[§] María José Ruiz,[†] and César Pastor[⊥]

Departamento de Química Inorgánica, Orgánica y Bioquímica, Facultad de Ciencias del Medio Ambiente, Universidad de Castilla−La Mancha, Avenida Carlos III, s/n 45071 Toledo, Spain, Departamento de Química Inorgánica, Orgánica y Bioquímica, Facultad de Químicas, Universidad de Castilla−La Mancha, Campus de Ciudad Real, 13071 Ciudad Real, Spain, Departamento de Química Inorgánica, Orgánica y Bioquímica, ETS Ingenieros Industriales, Universidad de Castilla−La Mancha, Avenida Camilo José Cela, 3, 13071 Ciudad Real, Spain, Institute of Chemical Research of Catalonia (ICIQ), Avenida Països Catalans 16, 43007 Tarragona, Spain, Departament de Química Física i Inorgànica, Universitat Rovira i Virgili, Avenida Marcel.lí Domingo s/n, 43007 Tarragona, Spain, and Servicio Interdepartamental de Apoyo a la Investigación, Facultad de Ciencias, Universidad Autónoma de Madrid, Spain

Received March 21, 2006

A series of new tantalum-digol (digol = diethylene glycolate) complexes TaCp*Cl_2(κ^3-digol) (**1**), TaCp*Me_2(κ^3-digol) (**2**), TaCp*ClMe(κ^3-digol) (**3**), and TaCp*Me(OTf)(κ^3-digol) (OTf = triflate) (**4**) have been synthesized. Treatment of **2** with 1 equiv of $H_2O{\cdot}B(C_6F_5)_3$ enabled the synthesis of a tantalum-oxo borane-stabilized complex, TaCp*{$O{\cdot}B(C_6F_5)_3$}(κ^3-digol) (**5**). Insertion processes into the methyl groups of complexes **2**, **3**, and **4** were not observed upon reaction with CO or isocyanides. In contrast, complex **4** reacted slowly with 1 equiv of xylylisocyanide (xylyl = 2,6-dimethylphenyl) to yield the dicationic aminocarbene complex [TaCp*{C(Me)NH(xylyl)}(OH_2)(κ^3-digol)][OTf]$_2$ (**6**). All products were characterized by NMR spectroscopy and elemental analysis. The single-crystal structures of **1**, **5**, and **6** were determined. The molecular structures of **1**, **2**, **3**, and **6** were also determined by means of DFT-based methods.

Introduction

Organometallic oxides[1] and alkoxides[2] play an important role in numerous catalytic processes[3] and also serve as molecular models for catalyst−substrate surface interactions.[4] It is equally significant that some of the earliest and best known organic−inorganic representatives, with extraordinary implications in the development of multifunctional materials, are certainly derived from these kinds of complexes.[5]

All of these interesting properties derive from the extreme versatility of alkoxide ligands, since appropriate substitution patterns allow for significant modification of the steric and electronic requirements.[6] More recently, chelating alkoxide ligands have become the focus of a great deal of attention as ancillary ligand frameworks for group 4 and 5 metal centers.[7] In recent years we have developed studies based on the synthesis of several families of cyclopentadienyl-containing early transition metal complexes with different types of assisted ligands, namely, pyrimidine alkoxide[8] and pyridyl alkoxide.[9] We are currently interested in studying the reactivity of monocyclopentadienyltantalum derivatives toward diethylene glycol (digol-H_2).[10] This ligand can perfectly surround metals, as three coordination sites are available: an alcoholate double function for charge neutralization and an oxygen-donor function to compensate the electronic demands of the metal ion. Surprisingly, the chemistry of poly(ethylene glycol) complexes is relatively unexplored; some compounds with lanthanides,[11]

* To whom correspondence should be addressed. E-mail: antonio.otero@uclm.es.

[†] Facultad de Ciencias del Medio Ambiente, Universidad de Castilla−La Mancha.

[‡] Facultad de Químicas, Universidad de Castilla−La Mancha.

[§] ETS Ingenieros Industriales, Universidad de Castilla−La Mancha.

[‖] Institute of Chemical Research of Catalonia (ICIQ) and Universitat Rovira i Virgili.

[⊥] Universidad Autónoma de Madrid.

(1) Roesky, H. W.; Haiduc, I.; Hosmane, N. S. *Chem. Rev.* **2003**, *103*, 2579.

(2) Bradley, D. C.; Mehrotra, R. C.; Singh, A.; Rothwell, I. P. *Alkoxo and Aryloxo Derivatives of Metals*; Academic Press: London, 2001.

(3) Sobota, P. *Coord. Chem. Rev.* **2004**, *248*, 1047.

(4) (a) Basset, J.-M.; Gates, B. C.; Candy, J. P.; Choplin, A.; Leconte, M.; Quignard, F.; Santini, C. *Surface Organometallic Chemistry: Molecular Approaches to Surface Catalysis*; Kluwer: Dordrecht, The Netherlands, 1988. (b) Coperet, C.; Chabanas, M.; Saint-Arroman, R. P.; Basset, J. M. *Angew. Chem., Int. Ed.* **2003**, *42*, 156.

(5) Sanchez, C.; Soler-Illia, G. J. de A. A.; Ribot, F.; Lalot, T.; Mayer, C. R.; Cabuil, V. *Chem. Mater.* **2001**, *13*, 3061.

(6) (a) Rothwell, I. P. *Acc. Chem. Res.* **1988**, *21*, 153. (b) Rothwell, I. P. *Chem. Commun.* **1997**, 1331.

(7) (a) Tshuva, E. Y.; Groysman, S.; Goldberg, I.; Kol, M. *Organometallics* **2002**, *21*, 662. (b) Tshuva, E. Y.; Goldberg, I.; Kol, M. *J. Am. Chem. Soc.* **2000**, *122*, 10706. (c) Shao, P.; Gendron, R. A. L.; Berg, D. J.; Bushnell, G. W. *Organometallics* **2000**, *19*, 509.

(8) Antiñolo, A.; Carrillo-Hermosilla, F.; Corrochano, A. E.; Fandos, R.; Fernández-Baeza, J.; Rodríguez, A. M.; Ruiz, M. J.; Otero, A. *Organometallics* **1999**, *18*, 5219.

(9) Fandos, R.; Hernández, C.; Otero, A.; Rodríguez, A. M.; Ruiz, M. J.; Terreros, P. *J. Chem. Soc., Dalton Trans.* **2000**, 2990.

(10) Abbreviations used: diethylene glycol = digol-H_2, diethylene glycolate = digol.

(11) (a) Hirashima, Y.; Shiokawa, J. *Chem. Lett.* **1979**, 463. (b) Hirashima, Y.; Tsutsui, T.; Shiokawa, J. *Chem. Lett.* **1981**, 1501. (c) Hirashima, Y.; Tsutsui, T.; Shiokawa, J. *Chem. Lett.* **1982**, 1405. (d) Hirashima, Y.; Kanetsuki, K.; Shiokawa, J.; Tanaka, N. *Bull. Chem. Soc. Jpn.* **1981**, *54*, 1567. (e) Hirashima, Y.; Kanetsuki, K.; Yonezu, I.; Kamakura, K.; Shiokawa, J. *Bull. Chem. Soc. Jpn.* **1983**, *56*, 738. (f) Rogers, R. D.; Voss, E. J.; Etzenhouser, R. D. *Inorg. Chem.* **1988**, *27*, 533.

10.1021/om060254e CCC: $33.50
Publication on Web 06/07/2006

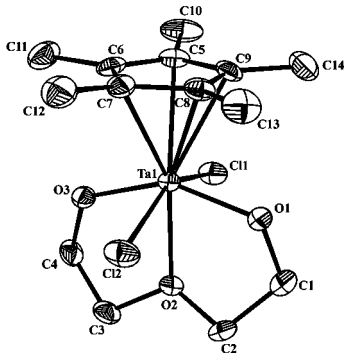

Figure 1. ORTEP drawing of compound **1** with thermal ellipsoids shown at 30% probability.

Scheme 1

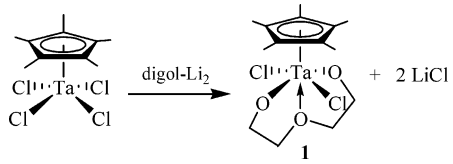

alkali and alkaline-earth metals,[12] and yttrium and titanium[13] have been reported, but to the best of our knowledge, only one organometallic complex of titanium containing this type of ligand has been described.[14]

We report here the synthesis, characterization, and theoretical studies of some monocyclopentadienyltantalum complexes containing the tridentate diethylene glycolate ligand. An interesting insertion reaction is also reported along with the formation of an aminocarbene dicationic complex.

Results and Discussion

The tantalum complex $TaCp^*Cl_4$ reacts with digol-Li_2 to yield complex **1**, which was isolated in good yield (70%) as a pale yellow solid (Scheme 1). This complex is air sensitive, rather soluble in THF and toluene, but sparingly soluble in pentane and Et_2O.

Complex **1** was characterized by the usual analytical and spectroscopic techniques. The ^1H NMR spectrum exhibits resonances at 2.21 (s), 3.63 (t), and 4.59 (t) ppm, and these are attributed to the Cp* ligand and the methylene protons of the dialkoxide ligand, respectively. The ratio of the integrals is consistent with the proposed stoichiometry. The multiplicity and number of methylene proton signals indicate a *trans* disposition of the chloride ligands and the coordination of the dialkoxide through the three oxygen atoms, with the central one in a *trans* disposition with respect to the Cp* ligand (see Scheme 1). The ^{13}C NMR spectrum is also consistent with the proposed structure.

This structure was also confirmed by an X-ray diffraction study. An ORTEP drawing of **1** is shown in Figure 1, and some selected bond distances and angles are given in Table 1. The crystal consists of discrete molecules separated by van der Waals distances. The tantalum atom is bonded to the cyclopentadienyl ring in a η^5-mode. The digol ligand is bonded to the metal center through the three oxygen atoms, two of which are located in the equatorial plane, *trans* to one another, and the central one occupying the position *trans* to the Cp* group. The coordination around the metal is best described as a pseudo-octahedral geometry, with the tantalum atom 0.557(1) Å out of the plane defined by the atoms Cl(1), Cl(2), O(1), and O(3). The Ta(1)−O(1) and Ta(1)−O(3) bond distances [1.950(7) and 1.934(6) Å, respectively] are within the normal range for tantalum alkoxide complexes.[15] The Ta(1)−O(2) bond length [2.212(6) Å] is longer and is comparable to that found previously by our group for similar ligands [2.375(6) Å].[16]

Table 1. Selected Bond Distances (Å) and Angles (deg) for $TaCp^*Cl_2(\kappa^3$-digol) Isomers

	mer			*fac*	
	X−ray[a]	calc		calc	
		Cp **1**-mer	Cp* **1**-mer*	Cp **1**-fac	Cp* **1**-fac*
Ta(1)−Cl(1)	2.457 (3)	2.473	2.483	2.462	2.469
Ta(1)−Cl(2)	2.488 (3)	2.525	2.514	2.455	2.460
Ta(1)−O(1)	1.950 (7)	1.953	1.962	1.973	1.982
Ta(1)−O(2)	2.212 (3)	2.257	2.282	2.383	2.467
Ta(1)−O(3)	1.934 (6)	1.955	1.969	1.966	1.981
Ta(1)−C(Cp)[b]	2.467 (4)	2.487	2.518	2.487	2.508
O(3)−Ta(1)−O(1)	147.9 (3)	147.5	147.1	96.9	98.2
O(3)−Ta(1)−O(2)	73.7 (3)	73.8	73.4	71.5	69.6
O(1)−Ta(1)−O(2)	74.2 (3)	73.9	73.7	71.5	70.7
O(3)−Ta(1)−Cl(1)	84.9 (2)	88.0	86.8	149.9	149.4
O(1)−Ta(1)−Cl(1)	87.2 (2)	87.5	86.8	84.0	83.4
O(2)−Ta(1)−Cl(1)	75.3 (18)	76.2	74.4	80.4	82.4

[a] X-ray specifications for $TaCp^*Cl_2(\kappa^3$-digol) (**1**). [b] Average Ta−C distances.

Scheme 2

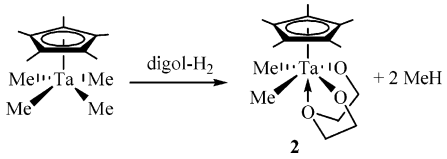

Another general way to achieve the synthesis of alkoxide derivatives of early transition metals is the reaction of metal alkyl complexes with alcohols to yield the corresponding alkanes and the alkoxide complexes. A likely mechanism for the protonolysis of the carbon−metal bond requires initial donation of an oxygen lone pair to the metal center.[17] This methodology has proven useful in the synthesis of alkyl/alkoxide tantalum complexes. For example, the tantalum complex $TaCp^*Me_4$ reacts with diethylene glycol in a 1:1 ratio to render complex **2**, which was isolated in 53% yield (see Scheme 2).

Complex **2** is air sensitive, rather soluble in THF and toluene, but sparingly soluble in pentane and Et_2O. This complex was characterized by ^1H and ^{13}C NMR and IR spectroscopy.

The ^1H NMR spectrum shows singlet signals at −0.03 and 1.91 ppm, which are assigned to the methyl groups bonded to the tantalum center and to the Cp* ligand, respectively. The methylene protons give rise to three multiplet signals centered at 2.85, 3.66, and 4.09 ppm. This situation is in contrast with the two triplets observed in complex **1**, where the two oxygen atoms were covalently bonded to the metal and the two chloro

(12) (a) Sieger, H.; Vogtle, F. *Tetrahedron Lett.* **1978**, *30*, 2709. (b) Singh, T. P.; Reinhardt, R.; Poonia, N. S. *Inorg. Nucl. Chem. Lett.* **1980**, *16*, 293. (c) Ohmoto, H.; Kai, Y.; Yasuoka, N.; Kasai, N.; Yanagida S.; Okahara, M. *Bull. Chem. Soc. Jpn.* **1979**, *52*, 1209.

(13) Sobota, P.; Utko, J.; Sztajnowska, K.; Jerzykiewicz, L. B. *New J. Chem.* **1998**, 851.

(14) Yi-Yeol, L.; Jin-Heong, Y. (Samsung General Chemicals Co., Ltd., S. Korea) Eur. Pat. Appl. EP964004, 1999.

(15) De Castro, I.; Galakhov, M. V.; Gómez, M.; Gómez-Sal, P.; Martín, A.; Royo, P. *J. Organomet. Chem.* **1996**, *514*, 51.

(16) Fandos, R.; Hernández, C.; López-Solera, I.; Otero, A.; Rodríguez, A. M.; Ruiz, M. J.; Terreros, P. *Organometallics* **2000**, *19*, 5318.

(17) Cardin, D. J.; Lappert, M. F.; Raston, C. L. *Chemistry of Organo-Zirconium and Hafmium Compounds*; Ellis Horwood Limited; Halsted Press: New York, 1986.

Scheme 3

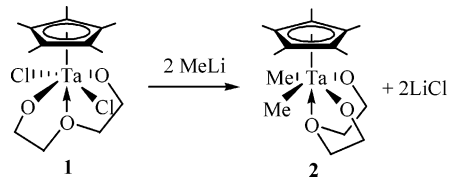

1 **2**

Scheme 4

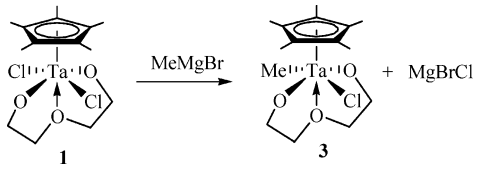

1 **3**

ligands were arranged in a *trans* fashion. Bearing this arrangement in mind, we propose that complex **2** is a monomer with the digol ligand bonded to the metal center in a *fac*[18] fashion in which the three oxygen atoms are bonded to the metal center and the two methyl groups are in a *cis* disposition (see Scheme 2).

The differences in the coordination modes of the digol ligand in **1** and **2** encouraged us to assess the preparation of a *trans*-dimethyl complex by methylation of compound **1**. As we envisaged, reaction of **1** with 2 equiv of MeLi in pentane gave only the *cis* dimethyl complex **2**, which was isolated in 63% yield (Scheme 3). Evidence for the formation of the *trans* complex was *not* found.

The use of other methylating agents such MeMgCl or MeMgI gave the *cis* complex **2** and $TaCp^*Me_4$ as the only identifiable compounds in the reaction mixture.

Finally, reaction of 2 equiv of MeMgBr with complex **1** gave the monomethylated complex **3**. When this reaction was repeated with only 1 equiv of MeMgBr, the same result was achieved and **3** was isolated in 46% yield as a pale yellow solid (Scheme 4).

This compound is soluble in toluene, THF, and acetonitrile but is sparingly soluble in pentane. The ^1H NMR spectrum shows two singlets at 0.11 and 2.07 ppm, and these are assigned to the methyl groups bonded to the tantalum atom and to the cyclopentadienyl ligand, respectively. Four multiplets are observed centered at 3.17, 4.17, 4.39, and 4.54, and these correspond to the nonequivalent protons of the digol ligand. In addition, the $^{13}C\{^1H\}$ NMR spectrum shows two signals at 72.4 and 74.1 ppm for the methylene carbons, which is consistent with a *mer* disposition of the oxygen atoms (see Scheme 4).

In complexes **1**, **3**, and **4** (see below) the digol ligand adopts the *mer* disposition, but in **2** it coordinates in the *fac* manner. A visual inspection of the X-ray structures suggests that the preference for coordination in the *fac* or *mer* arrangement was not determined by steric effects. In an effort to gain insight into this issue, the structures of the *fac* and *mer* isomers of **1**, **2**, and **3** were determined at a DFT level (see Computational Details and Supporting Information) considering both the Cp* ligands as used in the experiments and simple Cp ligands. Selected geometrical parameters for the computed structures of compound **1** are collected in Table 1. The agreement between X-ray measurements and computed values is fairly good. All metal−ligand bond distances are, however, slightly overestimated. In the case of compound **3**, the digol ligand can adopt two different conformations, **3**-*mer* and **3**-*mer*-*is*, as shown in the Supporting Information. At the present level of theory, the **3**-*mer* isomer is the most stable by 2.4 kcal·mol^{-1} and was therefore selected to evaluate the *mer*/*fac* relative stability.

Table 2. Relative Energy (kcal·mol^{-1}) of the *fac* and *mer* Isomers of 1, 2, and 3 for Cp and Cp* Ligands[a]

	$E_{fac} - E_{mer}$		
	1	**2**	**3**
Cp	9.9	−0.5	7.3
Cp*	8.2	−1.8	6.7

[a] A positive value indicates preference for the *mer* isomer.

The relative stabilities of the *fac* and *mer* isomers of compounds **1**, **2**, and **3** are shown in Table 2 for Cp and Cp* ligands. In all cases, the difference in energy agrees with the *mer*/*fac* selectivity described above. The thermodynamically most stable isomer (*mer* for **1** and **3**, and *fac* for **2**) matches that obtained experimentally. The trend arising from Table 2 indicates that the preference for the *mer* coordination mode is reduced as the number of chloride ligands decreases. This preference is ultimately reversed in **2**. It is worth noting that the preference for *mer* is enhanced when a Cp ligand, rather than a Cp*, is present. In **1** and **3** the energy differences between the two isomers are large enough to account for the experimental observation. Similar ΔE values for the *mer* and *fac* isomers of the related compound $V(O)(oda)(H_2O)_2$ [oda = $O(CH_2COO^-)_2$] have been reported.[19] However, in complex **2** the energy difference between the two isomers is quite small, less than 2 kcal·mol^{-1}, but the trend is in the right direction. Other cases reported in the literature show a similar type of behavior. For instance, Galindo and co-workers also found a small energy difference between the *fac* and *mer* isomers of the Ni(oda)-$(H_2O)_3$ derivative.[20] In a study on different systems, Harvey et al.[21] comprehensively explained the *cis*/*trans* preference in $[PtX_2(PR_3)_2]$ (X = Cl, Br, I, Me; R = H, F, Ph, Me) complexes. In that case, the *cis*/*trans* preference was determined by a range of effects that depended on X, R, and, to a great extent, the solvent. Those authors used a similar DFT methodology and found, for R = Me and in the gas phase, a preference of 6 kcal·mol^{-1} for *trans* when X = Cl and of 2 kcal·mol^{-1} for *cis* when X = Me. These results are almost reproduced by the values for compounds **1** and **2** in Table 2. In the present case, the stability of the *fac* isomer in **2** is probably driven by the preference of the strong sigma donor methyl ligands to bind *trans* to weaker ones.

A detailed analysis of the computed geometries of the isomers of **1**, **2**, and **3** shows that the Ta−Cl bond distances are longer than the Ta−Me bonds and the Ta−Cp distances do not change considerably. The Ta−O_2(ether) length increases with the number of methyl groups, in the order Cl > ClMe > Me_2, and in all cases the Ta−O_2(ether) distances are longer than the remaining Ta−O_1 and Ta−O_3. However, in all cases the existence of a Ta−O_2(ether) bond is confirmed by the presence of a bond critical point. Calculated geometrical parameters show that the *mer* **1**, **2**, and **3** isomers have shorter Ta−O_2(ether) distances than the *fac* compounds. In accordance with this, the *mer* isomers present a slightly higher electron density (0.06 e$^-$) than the *fac* derivatives (0.04 e$^-$) at the bond critical point.

The reactivity of $TaCp^*Me_2(\kappa^3$-digol) (**2**) with protonating reagents and unsaturated molecules was studied. Reaction with

(18) Albrecht, M.; van Koten, G. *Angew. Chem., Int. Ed.* **2001**, *40*, 3750.

(19) del Rio, D.; Galindo, A.; Vicente, R.; Mealli, C.; Ienco, A.; Masi, D. *J. Chem. Soc., Dalton Trans.* **2003**, 1813.

(20) Grirrane, A.; Pastor, A.; Ienco, A.; Mealli, C.; Galindo, A. *J. Chem. Soc., Dalton Trans.* **2002**, 3771.

(21) Harvey, J. N.; Heslop, K. M.; Orpen, G. A.; Pringle, P. G. *Chem. Commun.* **2003**, 278.

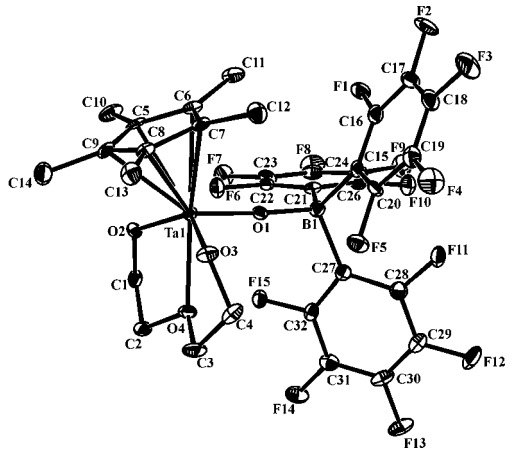

Figure 2. ORTEP drawing of compound **5** with thermal ellipsoids shown at 30% probability.

Scheme 5

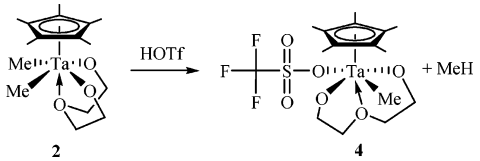

Scheme 6

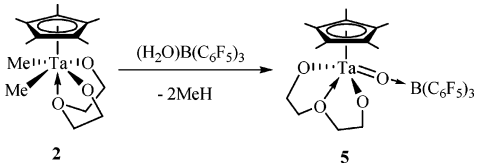

triflic acid occurs in a rather selective way to yield, through protonolysis of one tantalum−methyl bond, the corresponding alkyl complex **4** (Scheme 5).

This compound is soluble in toluene, THF, and acetonitrile but sparingly soluble in pentane, with this latter observation in agreement with its proposed neutral character. The NMR spectra show that, at room temperature, the methylene groups in the dialkoxide ligand are inequivalent and their signals appear in the ^{13}C spectrum at 71.9 and 74.5 ppm; this confirms the *mer* disposition of the digol ligand (see Scheme 5). The ^{1}H NMR spectrum shows singlet signals at −0.21 and 1.86 ppm, and these are attributed to the methyl groups bonded to the metal center and to the Cp* ligand, respectively, while the methylene groups give rise to several multiplets centered at 3.29, 3.85, 4.15, and 4.89 ppm.

We also studied the reaction of **2** with the water adduct $H_2O{\cdot}B(C_6F_5)_3$, which proved to be a useful oxo transfer reagent[22] and gave complex **5** in good yield (Scheme 6).

The molecular structure of compound **5** was determined by X-ray diffraction studies (Figure 2, Table 3). In this complex a tantalum oxo-borane adduct was formed. A related oxo-niobocene-borane adduct was previously reported by some of us.[23] The most notable feature of this compound, a Ta−O bond distance of 1.828(2) Å, is comparable to that in the reported mononuclear complex [TaCp*Cl_2{O·B(C_6F_5)$_3$}], 1.784(2) Å,[24] and even longer than those found in the compounds [TaCp*Cl(O){η^2-C(Me)=NR}] [1.731(7) Å][25] and [$TaCp_2$*H(O)] [1.73(2) Å].[26] This value for the Ta−O bond length is a consequence of the coordination of the oxygen atom to the borane ligand and is within the range of values found in complexes with Ta−O−Ta bridges [1.82−2.10 Å]. The O−B bond distance of 1.498(5) Å is shorter than that found for $H_2O{\cdot}B(C_6F_5)_3$ [1.5769(14) Å][27] but within the range observed for neutral oxo−borane compounds [1.496−1.591 Å].[28] The Ta−O−B angle deviates slightly from linearity [174.0(2)°], probably due to the steric requirements of the Cp* and $B(C_6F_5)_3$ ligands.

Table 3. Bond Lengths (Å) and Angles (deg) for 5

Ta(1)−O(1)	1.828(2)	B(1)−O(1)−Ta(1)	174.0(2)
Ta(1)−O(2)	1.946(2)	O(1)−Ta(1)−O(2)	107.25(11)
Ta(1)−O(3)	1.952(3)	O(1)−Ta(1)−O(3)	102.21(11)
Ta(1)−O(4)	2.313(2)	O(2)−Ta(1)−O(3)	130.41(11)
O(1)−B(1)	1.498(5)	O(1)−Ta(1)−O(4)	87.78(10)
O(2)−C(1)	1.421(5)	O(2)−Ta(1)−O(1)	70.90(10)
O(3)−C(4)	1.424(5)	O(3)−Ta(1)−O(4)	71.37(10)
O(4)−C(3)	1.444(5)		
O(4)−C(2)	1.449(5)		

Table 4. ^{19}F NMR Data in C_6D_6 at Room Temperature for Fluorine-Containing Compounds

compound	*ortho*	*para*	*meta*
$B(C_6F_5)_3$	−129.7	−142.6	−160.6
$H_2O{\cdot}B(C_6F_5)_3$	−135.4	−156.4	−163.9
TaCp*{O·$B(C_6F_5)_3$}(κ^3-digol) (**5**)	−133.7	−159.7	−165.6

Scheme 7

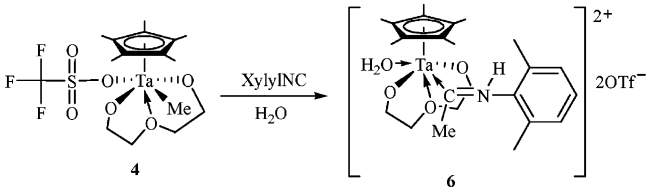

All of the spectroscopic data for compound **5** are in agreement with the structure described, but the ^{19}F NMR spectrum probably provides the most conclusive evidence. This spectrum shows resonances broadly similar to those of $B(C_6F_5)_3$, but the *para*-fluorine has shifted slightly upfield as in $H_2O{\cdot}B(C_6F_5)_3$ (see Table 4). This resonance is the most sensitive of the aromatic fluorine shifts and is a good indicator of tetracoordination of the boron atom.[29]

Insertion processes into the methyl groups of complexes **2**, **3**, and **4** were not observed upon reaction with CO or isocyanides, probably because the central oxygen atom in the digol ligand blocks the initial coordination of these molecules and prevents reactivity.

In contrast, complex **4** reacts slowly at room temperature (5 days) with 1 equiv of xylylisocyanide to yield the dicationic aminocarbene complex **6** (Scheme 7), probably by initial displacement of the triflate ligand by the isocyanide and subsequent protonation of the generated cationic iminoacyl (Scheme 8). Complex **6** was isolated as a colorless crystalline

(22) Neculai, D.; Roesky, H. W.; Neculai, A. M.; Magull, J.; Walfort, B.; Stalke, D. *Angew. Chem., Int. Ed.* **2002**, *41*, 4294.

(23) Antiñolo, A.; Carrillo-Hermosilla, F.; del Hierro, I.; Otero, A.; Fajardo, M.; Mugnier, Y. *Organometallics* **1997**, *16*, 4161.

(24) Sánchez-Nieves, J.; Frutos, L. M.; Royo, P.; Castaño, O.; Herdtweck, E. *Organometallics* **2005**, *24*, 2004.

(25) Gómez, M.; Gómez-Sal, P.; Jiménez, G.; Martín, A.; Royo, P.; Sánchez-Nieves, J. *Organometallics* **1996**, *15*, 3579.

(26) Parkin, G.; Asselt, A. V.; Leahy, D. J.; Whinnery, L.; Hua, N. G.; Quan, R. W.; Henling, L. M.; Schaefer, W. P.; Santarsiero, B. D.; Bercaw, J. E. *Inorg. Chem.* **1992**, *31*, 82.

(27) Danopoulos, A. A.; Galsworthy, J. R.; Green, M. L. H.; Cafferkey, S.; Doerrer, L. H.; Hursthouse, M. B. *Chem. Commun.* **1998**, 2529.

(28) (a) Barrado, G.; Doerrer, L.; Green, M. L. H.; Leech, M. A. *J. Chem. Soc., Dalton Trans.* **1999**, 1061. (b) Sarsfield, M. J.; Helliwell, M. *J. Am. Chem. Soc.* **2004**, *126*, 1036.

(29) Doerrer, L. H.; Green, M. L. H. *J. Chem. Soc., Dalton Trans.* **1999**, 4325.

Scheme 8

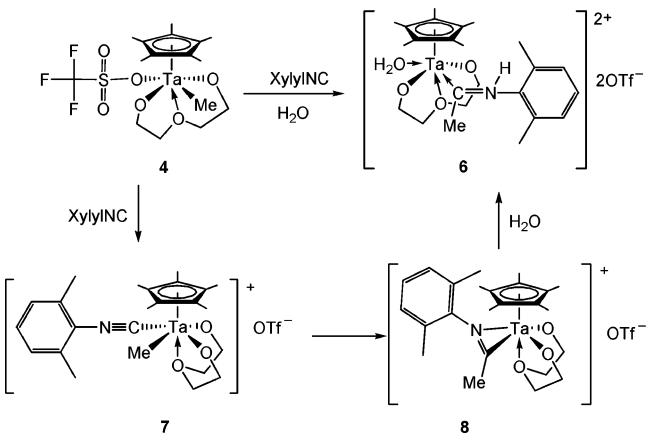

solid and was characterized by the usual analytical and spectroscopic techniques as well as by X-ray diffraction.

The mechanism of this transformation, i.e., methyl insertion into the xylylisocyanide (XylylNC)−Ta bond in [TaCp*(digol)(XylylNC)(Me)]$^+$ (**7**) to give [TaCp*(digol)η^2-(C,N)-(C(Me)-NXylyl)]$^+$ (**8**), as shown in Scheme 8, was investigated by means of DFT calculations using Cp ligands instead of Cp* and PhNC instead of XylylNC. We considered that the geometry of the active [TaCp(digol)(PhNC)(Me)]$^+$ (**7′**) intermediate corresponds to the *fac* isomer since the methyl insertion reaction is favored with the *cis* disposition of the two ligands. Molecular structures for **7′**, **8′**, and the corresponding transition state $\mathbf{TS}_{7'-8'}$ are displayed in Figure 3. Methyl insertion is thus energetically favorable, with the difference in energy between the [TaCp-(digol)(PhNC)(Me)]$^+$ and [TaCp(digol)η^2-(C,N)-(C(Me)NPh)]$^+$ being −26.2 kcal·mol^{-1}. The energy barrier to reach the transition state from **7′** amounts to only 11.8 kcal·mol^{-1}, a value that fully justifies the formation of **8′**. Characteristic interatomic distances are also given in Figure 3. The value of the angle Me−Ta−C decreases from 71° to 47° and the Me−C distance decreases to 1.862 Å in $\mathbf{TS}_{7'-8'}$, thus confirming the success of the insertion reaction. In the product **8′**, the C═N distance (1.292 Å) is characteristic of a double bond and the Me−C distance (1.485 Å) corresponds to a single C−C bond. The distance between the Ta atom and the C atom of the PhNC moiety decreased from 2.245 Å in the intermediate to 2.098 Å in the TS, whereas the Ta−Me distance increased from 2.262 to 2.494 Å.

Complex **6** is air stable in solution for several days and does not react with additional isocyanide; it is insoluble in toluene and pentane but is soluble in acetonitrile and THF, as one would expect given its cationic nature.

NMR data are in full agreement with the presence of an aminocarbene ligand in this complex, with the amino proton observed at 10.7 ppm in the ^{1}H NMR spectrum as a broad signal and the carbene carbon signal at 267.1 ppm in the ^{13}C NMR spectrum.[30] In addition, characteristic ν(N−H) and ν(O−H) absorptions were found at ∼3200 cm^{-1} in the IR spectrum. The bound H_2O molecule of **6** gives rise to a broad resonance at 2.45 ppm in the ^{1}H NMR spectrum and was further revealed by the solid-state structure determined crystallographically. An ORTEP drawing of **6** is shown in Figure 4, and some selected bond distances and angles are summarized in Table 5.

The crystal is formed by the cationic unit and two inequivalent triflate anions. In Figure 4 the anions have been omitted for clarity. The pentamethylcyclopentadienyl ring is bound to the Ta atom in an almost symmetric η^5-fashion with the distance between the metal and the centroid of the ring being 2.135(9) Å. The Ta atom is also bound to four oxygen atoms, with the Ta−O lengths ranging between 1.901(7) and 2.209(7) Å. Three oxygen atoms belong to a *mer*-κ^3-digol ligand. The coordination around Ta is completed by the carbenic C(5) atom from the aminocarbene ligand. The complex can be described as pseudo-octahedral, with the Ta atom displaced by 0.420(3) Å from the equatorial plane containing the atoms O(1), O(3), O(4), and C(5).

The Ta−OH_2 distance of 2.194(8) Å is shorter than Ta−O(2) [2.209(7) Å] and similar to that found in the literature for TaCp*(OH_2)(*p-tert*-butylcalix[4]arene) [2.188(3) Å].[31] The Ta-(1)C(5)N(1)C(7) moiety of the aminocarbene ligand is almost planar and is perpendicular to the phenyl ring [dihedral angle 87.2(8)°]; the bond distances are N(1)−C(5) [1.330(14) Å], N(1)−C(7) [1.467(15) Å], C(5)−C(6) [1.501(16) Å], and C(5)−Ta(1) [2.240(13) Å], and these are comparable to those found in other tantalum complexes with this type of ligand.[30]

The X-ray structure of **6** was taken as the starting point for a geometry optimization at the DFT level, adding the two undetected aquo hydrogen atoms and one proton attached to the nitrogen atom. The optimized bond distances and angles are generally overestimated in comparison with the experimental values. All of the Ta−O distances, including the Ta−OH_2 distance, are 0.03 Å longer than the values obtained in the X-ray study. Consequently, the nature of the aquo ligand is confirmed. The Ta−C(5) distance differs by only 0.05 Å in comparison to the experimental value and is characteristic of the aminocarbene ligand.

Moreover, the location of the N-bound hydrogen atom, which lies in the same plane as Ta(1)C(5)N(1)C(6), clearly indicates the aminocarbene nature of the ligand. Analysis of the electronic structure of this isolated moiety (see Supporting Information) clearly reveals a Fischer-type carbene; the difference in energy (computed at the same level as above) between the singlet and the triplet states favors the most stable singlet by 31.2 kcal·mol^{-1}, a value quite close to that reported recently for related (alkyl)(amino)carbenes.[32] The bonding mechanism between the aminocarbene and the metal fragment consists of donation from the carbene lone pair to an empty tantalum d orbital of appropriate symmetry. Metal-to-carbene π back-donation, even though orbitals of appropriate symmetry can interact effectively, does not contribute to bonding because of the lack of metal electrons.

Conclusions

The work described here concerned the synthesis of several monocyclopentadienyl complexes of tantalum with an assisted dialkoxide ligand, which exhibits a tridentate *fac* or *mer* coordination depending on the nature of the methyl- and chloro-substituents present in the molecule. DFT-based studies indicate that the preference for the *mer* coordination mode is reduced as the number of chloride ligands decreases, a finding in full agreement with experimental observations. A comparative theoretical study between Cp and Cp* derivatives indicates that the *fac*/*mer* selectivity is enhanced when the former ligand is used. Optimized metal−ligand bond distances are slightly overestimated, especially for the Cp* geometries. The Ta−O(ether) distance is longer than the Ta−O distances, and it

(30) Galakov, M. V.; Gómez, M.; Jiménez, G.; Royo, P.; Pellinghelli, M. A.; Tiripichio, A. *Organometallics* **1995**, *14*, 1901.

(31) Acho, J. A.; Doerrer, L. H.; Lippard, S. J. *Inorg. Chem.* **1995**, *34*, 2542.

(32) Canac, Y.; Conejero, S.; Donnadieu, B.; Schoeller, W. W.; Bertrand, G. *J. Am. Chem. Soc.* **2005**, *127*, 7312.

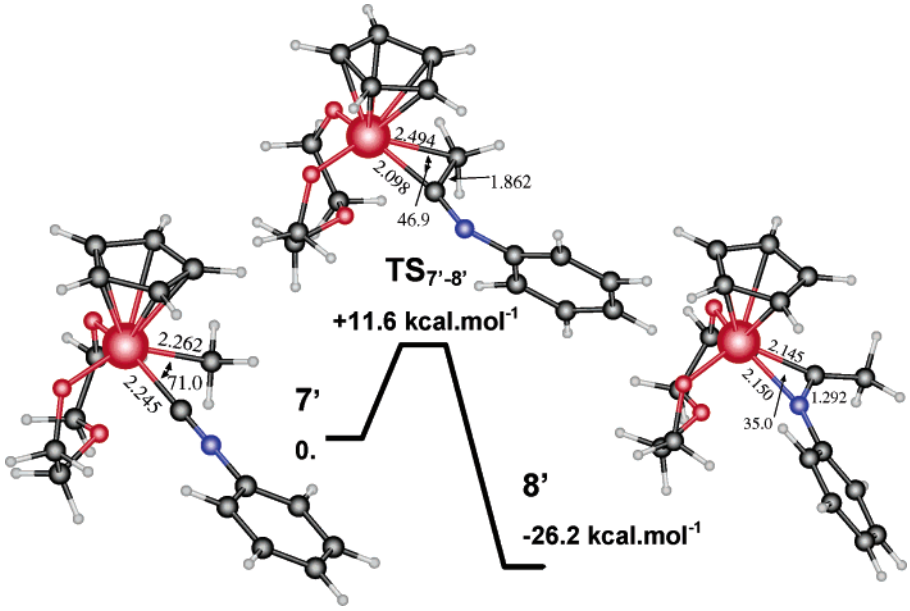

Figure 3. Molecular structures of **7′**, **TS**$_{7'-8'}$, and **8′** and relative energies. Selected distances in Å, angles in deg. The imaginary harmonic frequency for the TS is 410 cm^{-1}.

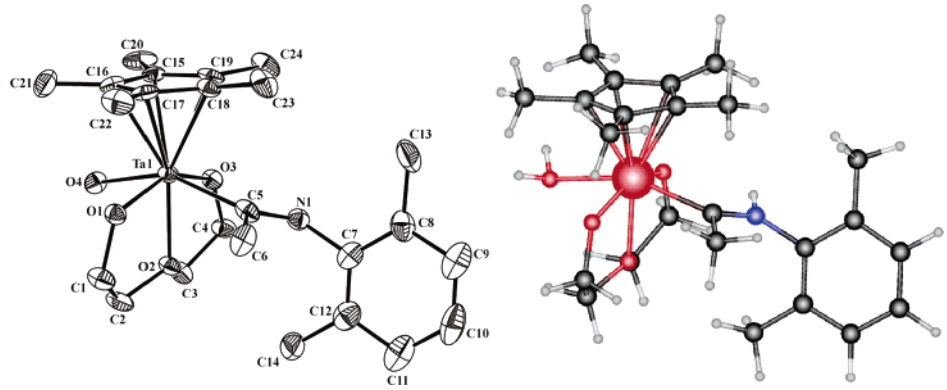

Figure 4. ORTEP drawing, with thermal ellipsoids shown at 30% probability, and molecular structure determined by DFT for **6**.

Table 5. Selected Bond Distances (Å) and Angles (deg) for Compound 6[a]

	X-ray	calc
Ta(1)−O(1)	1.898(6)	1.942
Ta(1)−O(2)	2.209(6)	2.256
Ta(1)−O(3)	1.920(6)	1.957
Ta(1)−O(4)	2.176(8)	2.362
Ta(1)−C(5)	2.24(1)	2.269
N(1)−C(5)	1.31(1)	1.316
N(1)−C(7)	1.47(1)	1.467
O(1)−Ta(1)−O(3)	147.2(3)	145.8
O(4)−Ta(1)−C(5)	153.1(3)	154.8
C(5)−N(1)−C(7)	127.0(9)	127.6
N(1)−C(5)−Ta(1)	123.5(7)	121.5
C(6)−C(5)−Ta(1)	121.7(7)	121.4

[a] X-ray specifications for [TaCp*{C(Me)NH(xylyl)}(OH$_2$)(κ^3-digol)][OTf]$_2$ (**6**).

becomes longer in the methylated compound **3**. The existence of a Ta−O(ether) bond is supported by the characterization of the Ta−O(ether) bond critical point in the electronic density distribution.

The reactivity of all of the methyl complexes with unsaturated molecules such as carbon monoxide or isocyanides was also studied. It was found that the central oxygen atom in the digol ligand probably blocks the initial coordination of these molecules and prevents reactivity. Only compound **4** reacted with xylylisocyanide, yielding a dicationic aminocarbene complex (**6**) instead of the expected neutral insertion compound. This reaction probably occurred by displacement of the triflate ligand. The mechanism of this transformation was determined by DFT calculations as well as the complete geometry of **6**. The computed geometry of **6** agrees well with X-ray structural parameters, confirming the nature of the aquo and aminocarbene ligands. The electronic study of **6** enabled the identification of this ligand as a Fischer-type carbene, and the bonding mechanism involves donation of the carbene lone pair to an empty Ta(V) d orbital.

Finally, a novel example showing the efficiency of $H_2O{\cdot}B(C_6F_5)_3$ as an oxo-transfer reagent has been found. It is important to note the potential role that the digol ligand, and other similar compounds, can play in modulating the structure and reactivity of early transition metal complexes. Further studies are currently being carried out.

Experimental Section

General Remarks. All compounds were prepared and handled with rigorous exclusion of air and moisture under a nitrogen atmosphere by using standard vacuum line and Schlenk techniques. All solvents were dried and distilled under nitrogen.

The following reagents were prepared by literature procedures:

$TaCp^*Cl_4$[33] and $TaCp^*Me_4$.[34] The commercially available compounds Cp*H, LiMe, MeMgBr, xylylisocyanide, *tert*-butylisocyanide, triflic acid, $H_2O{\cdot}B(C_6F_5)_3$, and diethylene glycol were used as received from Aldrich.

Elemental analyses were performed with a Perkin-Elmer 2400 microanalyzer. IR spectra were recorded in the region 4000−400 cm^{-1} with a Nicolet Magna-IR 550 spectrophotometer as Nujol mulls using PET cells. ^1H, ^{19}F, and ^{13}C NMR spectra were obtained on a 200 MHz Mercury Varian Fourier transform spectrometer. Trace amounts of protonated solvents were used as references, and chemical shifts are reported in units of parts per million relative to $SiMe_4$.

$TaCp^*Cl_2(\kappa^3$-digol) (1). To a solution of diethylene glycol (0.2 mL, 2.17 mmol) in diethyl ether (30 mL) at −78 °C was added ^{n}BuLi (1.6 M in hexane solution) (2.7 mL, 4.34 mmol). The mixture was allowed to reach room temperature and stirred for 15 min. The solution was cooled to −78 °C, and Cp^*TaCl_4 (0.993 g, 2.17 mmol) was added. The mixture was allowed to reach room temperature and stirred for 3 h. The solvent was removed under vacuum, the residue was extracted with toluene, and after filtration, the toluene was evaporated and the yellow oil washed with cold pentane to afford a pale yellow solid (0.752 g, 70%), which was characterized as **1**. Crystals of complex **1** that were suitable for X-ray diffraction were obtained by crystallization from toluene/pentane. IR (Nujol/PET) ν (cm^{-1}): 1109 (s), 1092 (s), 1029 (s), 927 (m), 545 (s). ^1H NMR (C_6D_6): δ 2.21 (s, 15 H, Cp*), 3.63 (t, $J = 5.67$ Hz, 4 H, CH_2O), 4.59 (t, $J = 5.67$ Hz, 4 H, CH_2O). $^{13}C\{^1H\}$ NMR (C_6D_6): δ 12.1 (Cp*), 73.2 (CH_2O), 74.3 (CH_2O), 125.1 (Cp*). Anal. Calcd for $C_{14}H_{23}Cl_2O_3Ta$ (491.18): C, 34.23; H, 4.72. Found: C, 34.22; H, 4.73.

$TaCp^*Me_2(\kappa^3$-digol) (2). This compound can be synthesized using either of the following methods.

(A) A solution of diethylene glycol (0.075 g, 0.71 mmol) in THF (1 mL) was added to a solution of Cp^*TaMe_4 (0.268 g, 0.71 mmol) in pentane at −78 °C. The mixture was allowed to reach room temperature and stirred for 3 h. The solvent was evaporated to dryness, and the resulting oily solid was washed with cold pentane (2 × 2 mL). The compound was dried to give an oily yellow solid (0.166 g, 53%), which was characterized as **2**. IR (Nujol/PET) ν (cm^{-1}): 1445 (m), 1372 (m), 1138 (s) 1090 (vs), 1033 (s), 920 (m), 907 (m), 516 (m) 474 (m). ^1H NMR (C_6D_6): δ −0.03 (s, 6 H, CH_3−Ta), 1.91 (s, 15 H, Cp*), 2.85 (m, 2 H, CH_2O), 3.66 (m, 2 H, CH_2O), 4.09 (m, 4 H, CH_2O). $^{13}C\{^1H\}$ NMR (C_6D_6): δ 11.1 (Cp*), 40.5 (CH_3−Ta), 66.6 (CH_2O), 73.27 (CH_2O), 117.5 (Cp*). Anal. Calcd for $C_{19}H_{29}O_3Ta$ (450.35): C, 42.67; H, 6.49. Found: C, 41.41; H, 5.71.

(B) To a solution of complex **1** (0.176 g, 0.36 mmol) in pentane (10 mL) was added MeLi (1.6 M in diethyl ether) (0.45 mL, 7.15 mmol). The mixture was stirred for 2 h, the solvent was removed under vacuum, and the residue was extracted with toluene (2 mL). The sample was dried to give an oily yellow solid (0.103 g, 63%), which was characterized as **2**.

$TaCp^*MeCl(\kappa^3$-digol) (3). To a solution of complex **1** (0.269 g, 0.55 mmol) in diethyl ether (10 mL) was added MeMgBr (3 M in diethyl ether) (0.20 mL, 0.55 mmol). The mixture was stirred for 30 min, the solvent was removed under vacuum, and the residue was washed with pentane (5 mL) to yield a pale yellow solid (0.163 g, 46%), which was characterized as $\mathbf{3}{\cdot}MgBrCl{\cdot}1/2Et_2O$. ^1H NMR (C_6D_6): δ 0.11 (s, 3H, CH_3−Ta), 2.07 (s, 15 H, Cp*), 3.17 (m, 2 H, CH_2O), 4.17 (m, 2 H, CH_2O), 4.39 (m, 2 H, CH_2O), 4.54 (m, 2 H, CH_2O). $^{13}C\{^1H\}$ NMR (C_6D_6): δ 12.0 (Cp*), 41.2 (CH_3−Ta), 72.4 (CH_2O), 74.1 (CH_2O), 121.8 (Cp*). Anal. Calcd for $C_{15}H_{26}BrCl_2MgO_3Ta{\cdot}1/2(C_4H_{10}O)$ (647.49): C, 31.51; H, 4.83. Found: C, 31.83; H, 4.98.

$TaCp^*Me(OTf)(\kappa^3$-digol) (4). To a solution of complex **2** (0.385 g, 0.85 mmol) in toluene (10 mL) was added triflic acid (78 μL, 0.85 mmol). The mixture was stirred for 30 min, the solvent was removed under vacuum, and the residue was washed with pentane (5 mL) to yield a white solid (0.208 g, 42%), which was characterized as **4**. ^1H NMR (C_6D_6): δ −0.18 (s, 3 H, CH_3−Ta), 1.87 (s, 15 H, Cp*), 3.29 (m, 2 H, CH_2O), 3.85 (m, 2 H, CH_2O), 4.15 (m, 2 H, CH_2O), 4.89 (m, 2 H, CH_2O). $^{13}C\{^1H\}$ NMR (C_6D_6): δ 11.0 (Cp*), 38.4 (CH_3−Ta), 71.9 (CH_2O), 74.5 (CH_2O), 122.5 (Cp*), 124.1 (CF_3). Anal. Calcd for $C_{16}H_{26}F_3O_6STa$ (584.38): C, 32.88; H, 4.48. Found: C, 32.73; H, 4.48.

$TaCp^*\{O{\cdot}B(C_6F_5)_3\}(\kappa^3$-digol) (5). To a solution of complex **2** (0.29 g, 0.64 mmol) in toluene (5 mL) was added $H_2O{\cdot}B(C_6F_5)_3$ (0.34 g, 0.64 mmol). The mixture was stirred for 4 h, the solvent was removed under vacuum, and the residue was dissolved in diethyl ether (5 mL). Slow diffusion of pentane into this solution gave a white microcrystalline solid (0.46 g, 75%), which was characterized as **5**. Crystals of complex **5** suitable for X-ray diffraction were obtained by recrystallization from diethyl ether/pentane. ^1H NMR (C_6D_6): δ 1.59 (s, 15 H, Cp*), 2.11 (m, 2 H, CH_2O), 2.96 (m, 2 H, CH_2O), 3.76 (m, 2 H, CH_2O), 4.05 (m, 2 H, CH_2O). $^{13}C\{^1H\}$ NMR (C_6D_6): δ 9.9 (Cp*), 69.9 (CH_2O), 73.3 (CH_2O), 123.6 (Cp*). ^{19}F NMR (C_6D_6): δ −133.7 (m, *ortho*), −159.7 (t, *para*), −165.6 (m, *meta*). Anal. Calcd for $C_{32}H_{23}BF_{15}O_4Ta$ (948.26): C, 40.53; H, 2.44. Found: C, 40.51; H, 2.72.

$[TaCp^*\{C(Me)NH(xylyl)\}(OH_2)(\kappa^3$-digol)$][OTf]_2$ (6). To a solution of complex **4** (0.246 g, 0.42 mmol) in toluene (3 mL) was added xylylisocyanide (0.055 g, 0.42 mmol). The mixture was stirred for 5 days, the solvent was evaporated to dryness, and the mixture was extracted with acetonitrile (2 mL). Removal of the solvent under vacuum and washing with diethyl ether (2 mL) gave **6** (0.114 g, 31%). Crystals of complex **6** suitable for X-ray diffraction were obtained by crystallization from acetonitrile/diethyl ether. ^1H NMR (CD_3CN): δ 2.23 (s, 3 H, CH_3−CN), 2.32 (s, 15 H, Cp*), 2.37 (s, 6 H, CH_3−xylyl), 2.45 (br, H_2O), 4.2−5.1 (mc, br, 8 H, CH_2O), 7.28−7.42 (m, 3 H, xylyl), 10.65 (br, NH). ^{19}F NMR (CD_3CN): δ −79.77. $^{13}C\{^1H\}$ NMR (CD_3CN): δ 11.1 (Cp*), 11.4 (CH_3-xylyl), 14.9 (CH_3−CN), 74.3 (CH_2O), 76.3 (CH_2O), 117.6 (Cp*), 124.3 (CF_3), 127.4 (ar), 130.0 (ar), 133.4 (*ipso*-CH_3), 136.5 (*ipso*-CN), 267.1 (CN). Anal. Calcd for $C_{26}H_{38}F_6NO_{10}S_2Ta$ (882.64): C, 35.58; H, 4.23; N, 1.59. Found: C, 35.41; H, 4.08; N, 1.85.

Computational Details

All DFT calculations were carried out using the Amsterdam Density Functional (ADF2004.01) program developed by Baerends et al.[35] and vectorized by Ravenek.[36] The numerical integration scheme applied for the calculations was developed by te Velde et al.[37] The geometry optimization procedure was based on the method reported by Versluis and Ziegler.[38] The BP86 functional described as a combination between local VWN exchange−correlation potential with nonlocal Becke's exchange correction[39] and Perdew's correlation correction were used.[40] Relativistic corrections were introduced by scalar-relativistic zero-order regular approximation

(33) Burt, R. J.; Chatt, J.; Leigh, G. J.; Teuben, J. H.; Westerhof A. *J. Organomet. Chem.* **1977**, *129*, C33.

(34) Sanner, R. D.; Carter, S. T.; Burton, W. J. *J. Organomet. Chem.* **1982**, *240*, 157.

(35) (a) Baerends, E. J.; Ellis, D. E.; Ros, P. *Chem. Phys.* **1973**, *2*, 41. (b) Baerends, E. J.; Ros, P. *Chem. Phys.* **1973**, *2*, 52.

(36) Ravenek, W. In *Algorithms and Applications on Vector and Parallel Computers*; te Riele, H. J. J., Deckker, T. J., van de Horst, H. A., Eds.; Elsevier: Amsterdam, The Netherlands, 1987.

(37) (a) Boerrigter, P. M.; te Velde, G.; Baerends, E. J. *Int. J. Quantum Chem.* **1988**, *33*, 87. (b) te Velde, G.; Baerends, E. J. *J. Comput. Chem.* **1992**, *99*, 84.

(38) Versluis, L.; Ziegler, T. *J. Chem. Phys.* **1988**, *88*, 322.

(39) Becke, A. D. *Phys. Rev. A* **1988**, *38*, 3098.

(40) Perdew, J. P. *Phys. Rev. B* **1986**, *34*, 7406. Perdew, J. P. *Phys. Rev. B* **1986**, *33*, 8822.

Table 6. Crystal Data and Structure Refinement for 1, 5, and 6

	1	5	6
empirical formula	$C_{14}H_{23}Cl_2O_3Ta$	$C_{32}H_{23}BF_{15}O_4Ta$	$C_{24}H_{38}NO_4Ta{\cdot}2CF_3SO_3$
fw	491.17	948.26	883.64
temperature (K)	290(2)	100(2)	290(2)
wavelength (Å)	0.71073	1.54178	0.71073
cryst syst	monoclinic	triclinic	monoclinic
space group	$P2_1/n$	$P\bar{1}$	$P2_1/n$
a (Å)	10.060(2)	9.4230(1)	10.414(2)
b (Å)	12.410(1)	11.2053(1)	25.139(4)
c (Å)	13.713(5)	16.6550(1)	12.841(7)
α (deg)		75.192(1)	
β (deg)	105.13(2)	73.809(1)	94.36(3)
χ (deg)		78.027(1)	
volume (Å^3)	1652.6(7)	1615.06(2)	3352(2)
Z	4	2	4
density(calcd) (g/cm^3)	1.974	1.950	1.751
abs coeff (mm^{-1})	6.978	7.445	3.489
F(000)	952	920	1760
cryst size (mm^3)	0.22 × 0.20 × 0.20	0.18 × 0.14 × 0.08	0.20 × 0.10 × 0.10
θ range for data collection (deg)	2.25 to 28.04	2.83 to 62.73	2.12 to 27.96
index ranges	$-13 \le h \le 12$	$-10 \le h \le 10$	$-13 \le h \le 13$
	$0 \le k \le 16$	$-12 \le k \le 11$	$0 \le k \le 33$
	$0 \le l \le 18$	$-19 \le l \le 17$	$0 \le l \le 16$
no. of reflns collected	4101	9766	8392
indep reflns	3946 [R(int) = 0.0265]	4814 [R(int) = 0.0302]	8055 [R(int) = 0.0619]
no. of data/restraints/params	3946/0/186	4814/0/570	8055/99/457
goodness-of-fit on F^2	1.004	1.038	0.998
final R indices [$I > 2\sigma(I)$]	R1 = 0.0231, wR2 = 0.0474	R1 = 0.0261, wR2 = 0.0657	R1 = 0.0606, wR2 = 0.1160
largest diff peak and hole (e·Å^{-3})	0.760 and −0.822	0.989 and −0.490	1.272 and −1.386

(ZORA).[41] A triple-ζ plus two polarization basis set was used for tantalum atoms and a plus one polarization function for the other atoms. For non-hydrogen atoms a relativistic frozen-core potential was used, including 4d for tantalum, 2p for chlorine, and 1s for carbon and oxygen. A numerical integration parameter of 5.0 was employed in optimization and single-point calculations. Geometry convergence criteria were raised 1 order of magnitude to 10^{-3} hartree·Å^{-1}. Symmetry constraints were not used. The topological analysis of the electron density function was carried out using the Xaim program package.[42]

X-ray Data Collection, Structure Determination, and Refinement of Complexes 1, 5, and 6. The crystallographic data and experimental details about the data collection and structure refinement are listed in Table 6. The crystals of compounds **1** and **6** were selected and mounted on a fine glass fibber with epoxy cement. The data collections were performed at 25 °C on a Nonius-Mach3 diffractometer equipped with a graphite-monochromated radiation source (λ = 0.71073 Å) using a $\omega/2\theta$ scan technique to a maximum value of 56°. Unit cell dimensions were obtained by a least-squares fit of the 2θ values of 25 high-order reflections by using the Mach3 centering routines. Data were corrected in the usual fashion for Lorentz and polarization effects, and a semiempirical absorption correction was not necessary.

A single crystal of **5** was mounted on a glass fiber and transferred to a Bruker SMART 6K CCD area-detector three-circle diffractometer with a MAC Science rotating anode (Cu Kα radiation, λ = 1.54178 Å) generator equipped with Goebel mirrors at settings of 50 kV and 100 mA. X-ray data were collected at 100 K, with a combination of six runs at different φ and 2θ angles, 3600 frames. The data were collected using 0.3° wide ω scans (1 s/frame at 2θ = 40° and 2 s/frame at 2θ = 100°), with a crystal-to-detector distance of 4.0 cm. The substantial redundancy in data allows empirical absorption corrections (SADABS[43]) to be applied using multiple measurements of symmetry-equivalent reflections (ratio of minimum to maximum apparent transmission: 0.7013). The unit cell parameters were calculated and refined from the full data set. The raw intensity data frames were integrated with the SAINT[44] program, which also applied corrections for Lorentz and polarization effects.

For all three compounds, the software package SHELXTL[45] version 6.10 was used for space group determination, structure solution, and refinement. The structure was solved by direct methods (SHELXS-97),[46] completed with difference Fourier syntheses, and refined with full-matrix least-squares using SHELXL-97[47] minimizing $w(F_o^2 - F_c^2)^2$. Weighted R factors (R_w) and all goodness of fit S are based on F^2; conventional R factors (R) are based on F. All non-hydrogen atoms were refined with anisotropic displacement parameters. All scattering factors and anomalous dispersions factors are contained in the SHELXTL 6.10 program library. The hydrogen atom positions were calculated geometrically and were allowed to ride on their parent carbon atoms with fixed isotropic U, except H100 and H101 for **6**, which were located in the difference Fourier map and subsequently fixed.

Acknowledgment. Some of us (R.F., C.H., A.O., A.R., M.J.R.) gratefully acknowledge financial support from the Ministerio de Educación y Ciencia, Spain (Grant No. BQU2002-04638-CO2-02) and the Junta de Comunidades de Castilla−La Mancha (Grant Nos. PAC-02-003 and GC-02-010). C.B. and M.F. are indebted to the ICIQ Foundation for financial support.

(41) (a) van Lenthe, E.; Baerends, E. J.; Snijders, J. G. *J. Chem. Phys.* **1993**, *99*, 4597. (b) van Lenthe, E.; Baerends, E. J.; Snijders, J. G. *J. Chem. Phys.* **1994**, *101*, 9783. (c) van Lenthe E.; Ehlers, A.; Baerends, E. J. *J. Chem. Phys.* **1999**, *110*, 8943.

(42) Ortiz Alba, J. C.; Bo, C. *Xaim-1.0*; Universitat Rovira I Virgili: Tarragona, Spain. http://www.quimica.urv.es/XAIM.

(43) Sheldrick, G. M. *SADABS version 2.03, A Program for Empirical Absorption Correction*; Universität Göttingen, 1997−2001.

(44) *SAINT+ NT ver. 6.04, SAX Area-Detector Integration Program*; Bruker AXS: Madison, WI, 1997−2001.

(45) *Bruker AXS SHELXTL version 6.10, Structure Determination Package*; Bruker AXS: Madison, WI, 2000.

(46) Sheldrick, G. M. *SHELXS-97, Program for Structure Solution*: *Acta Crystallogr. Sect. A* **1990**, *46*, 467.

(47) (a) Sheldrick, G. M. *SHELXL-97, Program for Crystal Structure Refinement*; Universität Göttingen, 1997. (b) *SMART v. 5.625, Area-Detector Software Package*; Bruker AXS: Madison, WI, 1997−2001.

M.F. thanks the Torres Quevedo program of the Ministerio de Educación y Ciencia, Spain.

Supporting Information Available: Cartesian coordinates (in Å) of the structures considered in this study, molecular structures of **2** and **3**, selected geometrical parameters, interaction diagram of molecular orbitals of **6**, and CIF files for **1**, **5**, and **6**. This material is available free of charge via the Internet at http://pubs.acs.org.

OM060254E